

Inter-comparison of aerosol optical depth from the Multi-Wavelength Solar Radiometer with other radiometric measurements

Sobhan Kumar Kompalli, S Suresh Babu^{§,*} & K Krishna Moorthy

Space Physics Laboratory, Vikram Sarabhai Space Center, Thriuvananthapuram 695 022, India

[§]E-mail: s_sureshbabu@vssc.gov.in

Received 31 May 2010; revised received and accepted 23 November 2010

The Multi-Wavelength Solar Radiometer (MWR), designed and developed in the Space Physics Laboratory, has been extensively used by several research institutions across the country for estimating columnar spectral aerosol optical depth (AOD), the most important parameter needed for assessing the impact of aerosols on regional aerosol forcing. A network of > 30 MWRs is currently in operation under the Aerosol Radiative Forcing over India (ARFI) Project of Indian Space Research Organization's Geosphere Biosphere Program (ISRO-GBP). This paper reports the results of an extensive inter-comparison of the AODs deduced using the MWR with those obtained from other commercially available instruments, such as a Multi-Filter Rotating Shadowband Radiometer (MFRSR), a calibrated Microtops Sun Photometer (MTOPOS) and an EKO Sun Photometer (ESP). The results indicated very good agreement between the AOD derived from MWR with MFRSR, MTOPOS and ESP with correlation coefficients of ~ 0.99, 0.88 and 0.92, respectively. This report is intended to serve as a reference document for researchers while using the MWR along with other commercial instruments.

Keywords: Aerosol optical depth, Multi-Wavelength Solar Radiometer (MWR), Aerosol Radiative Forcing over India (ARFI)

PACS No.: 92.60.Mt

1 Introduction

The influence of atmospheric aerosols on the earth's radiation budget through their direct and indirect radiative forcing and the resulting climate implications remains largely uncertain due to their vast heterogeneity in spatial and temporal domain. Realizing the importance in the regional characterization of atmospheric aerosols for reducing their current uncertainties, a network of ground-based aerosol observatories are being established across the length and breadth of India, having distinct geographical features, under the Aerosol Radiative Forcing over India (ARFI) project of the Indian Space Research Organization's Geosphere Biosphere Program (ISRO-GBP). The Multi-Wavelength Solar Radiometer (MWR), designed and developed in house at the Space Physics Laboratory (SPL) of the Vikram Sarabhai Space Centre (VSSC), has been extensively used by several research institutions across the country for estimating columnar spectral aerosol optical depth (AOD), the most important parameter needed for assessing the impact of aerosols on regional aerosol forcing. A network of >30 MWRs is currently in operation under this ARFI network as

shown in Fig. 1. Before the deployment at a network station, each MWR is tested for integrity with the master MWR at SPL and excellent spectral agreement is ensured with statistical significance better than 99.5%.

The columnar AOD determines the total extinction caused by the aerosols distributed in a vertical column of the atmosphere. The magnitude of aerosol radiative forcing at any location and time depends on the AOD, aerosol properties, their vertical distribution, underlying surface albedo and solar zenith angle¹. Since, usually AOD varies on regional scales more than the other aerosol quantities involved, it is of first order importance to have a reliable regional database of AOD. In order to estimate AOD, different instrumentations are being used worldwide as part of several national and international efforts²⁻⁴. However, the basic principle for retrieving AOD is the same for most of the techniques, which follow the most common Beer-Lambert-Bouguer Law. The comparability of data emanating from these various instruments is indispensable in order to have concurrence among measurements and to form a reliable global database. Several studies⁵⁻⁷ have



Fig. 1 — The ARFI network over India

already pointed out the importance of inter-comparability for evaluation of data quality and the improvement of the retrieval procedures. Closure experiments to establish the consistency of various instruments measuring the same aerosol property and quantifying the long-term trends from such dependable databases are needed for accurate estimation of regional as well as global radiative forcing⁸. In the present work, the MWR retrieved spectral AOD has been compared with those estimated using three other commercially available instruments, viz. Multi-Filter Rotating Shadowband Radiometer (MFRSR), Microtops Sun Photometer (MTOPS) and EKO Sun Photometer (ESP).

2 Databases

Collocated measurements of spectral AOD by using MWR and MFRSR were carried out at Thumba (8.55°N, 76.97°E, 3 m msl) between December 2008 and February 2009 (21 days) on days when unobstructed solar visibility (the line of sight between the instrument and the sun is cloud free) was available for at least three hours a day. Concurrent measurements of AOD by MWR and MTOPS were carried out on the cloud free days from Port Blair

(11.63°N, 92.71°E, an island location in the Bay of Bengal) between January and March 2002 (20 days). Supplementing the above data, 11 days of MWR and MTOPS observations were also carried out from Thumba between January and March 2009. The data collected during the period January - April 1998 (38 days) during Intense Field Phase (IFP) of the Indian Ocean Experiment (INDOEX) onboard ORV Sagar Kanya⁹ over the Indian Ocean and Arabian Sea were used to inter-compare the MWR observations with EKO Sun Photometer (ESP).

3 Instrument details and operational principles

All four instruments, viz. MWR, MFRSR, MTOPS and ESP, used in the present investigations are ground-based passive remote sensing instruments which measure directly transmitted ground reaching solar flux as a function of wavelength. The Langley technique¹⁰ is used to estimate spectral AOD in the case of MWR, MFRSR and ESP; whereas MTOPS derived AOD is based on its internal calibration coefficients. In the Langley plot technique for the estimation of total optical depth of the atmosphere, the natural log of the direct normal irradiance (measured in mV as a function of time) is plotted

against the relative air mass obtained from the information of the optical path length of the direct solar beam through the atmosphere for various times of the day. The slope of the linear least square fit of the data points gives the total optical depth. AOD is extracted from this by subtracting the contribution from all other absorbing and scattering sources other than aerosols. In the present analysis, 99% confidence bands are estimated for the data points, for each set of data points separately at different wavelengths. The data points, which lie outside this band, are rejected as outliers and have not been included for the determination of final values of optical depths. The temporal stability of the extrapolated intercept of the Langley plot with zero air mass is used to ascertain the stability of the instrument. The common and unique features of all the instruments along with their specifications are given in Table 1.

3.1 Multi-Wavelength Solar Radiometer (MWR)

The MWR is a filter wheel radiometer and provides continuous measurements of directly transmitted, ground reaching solar flux at ten narrow wavelength bands centered at 380, 400, 450, 500, 600, 650, 750, 850, 935 and 1025 nm in a sequence, as a function of solar zenith angle, from which spectral AODs are calculated following Langley technique¹⁰. The channel 935 nm has strong absorption due to water vapour and this channel is mainly used for estimating columnar water vapour along with the window channel 1025 and this information is used to correct for water vapour absorption at 850 nm (which is very small, ~0.005 typically). As far as the absorption due to ozone (O₃) is concerned, the maximum contribution to AOD works out to be 0.03 at 600 nm (close to the peak of the Chappius band). The optical depth due to O₃ absorption as a function of wavelength is estimated for the wavelength range 450 - 700 nm using spectral absorption cross section from LOWTRAN (at 5 cm⁻¹

resolution) and model altitude profile of O₃ for Indian regions derived from rocket and balloon measurements. The uncertainties in these are very small (< 0.003).

The bands are selected using the narrow band interference filters with nominal full width and half maximum (FWHM) bandwidths of 5 nm and a band shape factor 3, which ensures a near uniform transmittance within the pass band and a sharp reduction in the transmission beyond. The filters are blocked beyond the pass band, from far UV to far IR, and the transmission in the blocking range is < 10⁻⁴ of that in the pass band. The band selected radiation is passed through a field limiting optics that limits the total field of view of the MWR to < 2°. The radiation is detected using a photo detector amplifier hybrid (UDT 455 UV of United detector technology) operating in photovoltaic mode. The output voltage of the UDT is proportional to flux incident at the entrance window, over several orders of intensity variations. This voltage is digitized using a 12-bit ADC and the data is recorded on to an IBM compatible PC along with the information of the wavelength and time of observation (accurate to 1 second). The instrument operates in a fully automatic mode employing a passive equatorial mount and the data are collected sequentially in each wavelength band at regular intervals of 2 min over the entire wavelength range using a filter wheel assembly.

In the estimation of AOD by the Langley technique, the stability of the instrument is important. This is ascertained by examining the temporal invariability of the Langley intercept, corrected for the daily variation in Sun-Earth distance. The long-term stability of the instrument was fairly good, with the Langley intercepts lying within 5% of the mean typically. The fluctuations are relatively higher at the shorter wavelengths compared to those at the longer wavelengths. Estimates have shown that typical error

Table 1 — Specification details of MWR, MFRSR, MTOPS and ESP

Specification	MWR	MFRSR	MTOPS	ESP
Measurement	Direct	Total, diffuse, direct	Direct	Direct
Operation	Automatic, Sun tracking	Automatic, Shadowband	Handheld, Sun pointed	Hand held, Sun pointed
No. of channels	10	7	5	4
Central wavelengths, nm	380, 400, 450, 500, 600, 650, 750, 850, 935, 1025	Total 300-1100, 417.9, 496.8, 627.3, 691.2, 870.4, 939.4	440, 500, 675, 870, 935	368, 500, 675, 778
Bandwidth FWHM	5 nm	10 nm	10 nm	5 nm
Field of View	2°	3.3°	2.5°	2.4°

in the retrieved AOD is ~ 0.01 excluding the variance of the Langley intercept. The variance of the Langley intercept along with the other uncertainties puts the uncertainty in AOD in the range of 0.02–0.03 at different wavelengths, the values tending toward the upper levels at shorter wavelengths (< 500 nm) and during periods of high AODs (> 0.5). Thus, these uncertainties are for the worst case and also account for the effects of averaging and statistical (regression) analysis.

3.2 Multi-Filter Rotating Shadow band Radiometer (MFRSR)

The MFRSR is a widely used instrument for AOD retrievals, which measures total, diffuse and direct flux of incoming solar radiation. It consists of a horizontal circular aperture covered by a white diffuser disc, and a rotating shadow band that shades the diffuser with an umbral angle of 3.3° , in regular intervals controlled by an ephemeris calculation. After passing through the diffuser surface, the radiation is sensed by 7 silicon detectors: a total channel and other six spectral channels having 10 nm FWHM, centered at 417.9, 496.8, 627.3, 691.2, 870.4 and 939.4 nm. Time series of direct solar beam extinctions and horizontal diffuse flux are derived from four actual measurements: the total horizontal irradiance with the shadow band located under the diffuser not blocking any light; and the other one the Sun blocked measurement; thus, the MFRSR alternatively measures the total and diffuse irradiance falling on a horizontal surface. Two side band measurements, with shadow band blocking a section of the sky 9° east and west, respectively from the Sun are used to estimate the fraction of the diffused flux blocked by the shadow band during the diffuse measurement. The described four measurements (in mV) are combined into the diffuse horizontal and direct horizontal measurements. The later is normalized into the direct normal flux by dividing with cosine of solar zenith angle and the pre-determined angular response correction applied for the imperfect cosine response of the quasi-Lambertian receiver. The spectral AOD is retrieved from the direct normal flux following the Langley technique. The details of the instrument, its uncertainties and calibration procedure are well discussed in the literature¹¹⁻¹⁴.

3.3 Microtop Sun Photometer (MTOPS)

Microtop is a simple, compact, hand held, easy to use sun photometer, manufactured by the Solar Light Company, USA, specifically for field experiments. It

estimates AOD from individual/spot measurements following the Beer-Lambert-Bouguer law¹⁵⁻¹⁶, which adds an important advantage when the sky is partly clear for short duration and on the moving platforms. Microtop measures the solar irradiance in five, user selectable, spectral wave bands (440, 500, 675, 870 and 936 nm in this study) from which it derives AOD based on its internal calibration coefficients. The filters used in all channels have a peak wavelength precision of ± 1.5 nm and a full width at half maximum (FWHM) band pass of 10 nm. The system uses photodiode detectors coupled with amplifiers and A/D converters. The collimators are mounted in a cast aluminum block with a full field of view of 2.5° . The instrument has built-in pressure and temperature sensors and allows for a GPS connection to obtain the position and time. The cross hairs and two concentric circles in the sun-centering view window help the user point the instrument directly to the Sun.

3.4 EKO Sun Photometer (ESP)

EKO Sun Photometer¹⁷ (ESP, Model MS-120 of EKO Instruments Trading Company Ltd, Japan) is a handheld, manually operated filter wheel radiometer with a field of view of 2.4° . It consists of four channels with peak wavelengths at 368, 500, 675 and 778 nm with a bandwidth of 5-6 nm. When the system points directly towards the sun, the sample and hold circuitry of the system holds the peak signal voltage and the output voltage is displayed on the LCD. The accurate alignment towards the sun is facilitated by coinciding the image of the Sun formed by a pinhole, on a crosswire in a small window of the instrument. Each filter is brought into the field of view by turning a thumbwheel and the output signal (maximum) is recorded against the time, which the operator has to note down along with the output of the ESP for each filter. This forms the raw data, from which optical depth is deduced using the Beer-Lambert-Bouguer law without any absolute calibration of the instrument.

4 Results and Discussions

4.1 Time series of AOD

The time series of AOD at 500 nm retrieved from MFRSR (τ_{MFRSR}), MTOPS (τ_{MTOPS}) and ESP (τ_{ESP}) observations with the respective concurrent measurements of MWR (τ_{MWR}) is examined in Fig. 2 (a-c). It is evident from the figures that the MWR derived AODs follow the same temporal variation with those derived from other instruments. It

has already been mentioned that both MFRSR and ESP use the Langley technique as is the case for the MWR for the estimation of AOD, whereas MTOPS derived AOD is based on internal calibration constants.

During the period of MWR and MFRSR observations, high AOD values (e.g. $\tau_{\text{MWR}} = 0.57$ on 24 January 2009) to moderate AOD values (e.g. $\tau_{\text{MWR}} = 0.23$ on 19 January 2009) prevailed as clearly noted in Fig. 2(a). The mean values were $\tau_{\text{MWR}} \sim 0.4 \pm 0.10$ and $\tau_{\text{MFRSR}} \sim 0.42 \pm 0.10$. On the other hand,

showed [Fig. 2 (b)] moderate AOD values with mean values of $\tau_{\text{MWR}} \sim 0.33 \pm 0.08$ and $\tau_{\text{MTOPS}} \sim 0.35 \pm 0.09$. The MWR and ESP observations also showed [Fig. 2(c)] strong temporal variations ranging from a very high value of ~ 0.57 to as low as ~ 0.01 , with a mean value of $\tau_{\text{MWR}} \sim 0.21 \pm 0.1$ and $\tau_{\text{ESP}} \sim 0.22 \pm 0.10$.

4.2 Inter-comparison of AODs

With a view to quantifying the association between AODs estimated from various instruments, the statistical parameters, viz. mean bias difference

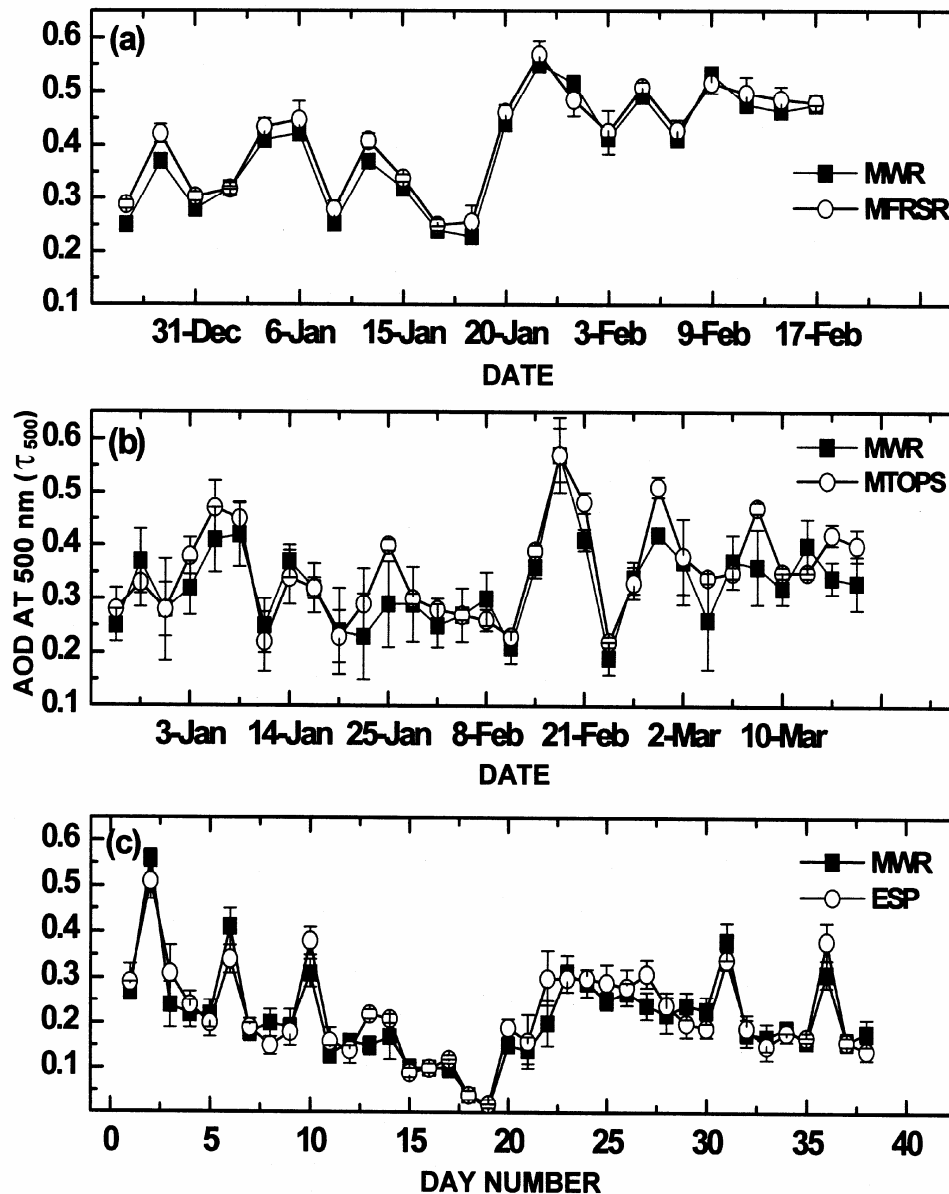


Fig. 2 — Time series of AOD at 500 nm with respect to different observations: (a) MWR vs MFRSR; (b) MWR vs Microtops Sun Photometer; (c) MWR vs EKO Sun Photometer

(MBD), root mean square difference (RMSD) and absolute percentage deviation (APD) were computed using the following relations⁷:

$$MBD = N^{-1} \sum_i^N (X_i - MWR_i) \quad \dots (1)$$

$$RMSD = \left[N^{-1} \sum_i^N (X_i - MWR_i)^2 \right]^{0.5} \quad \dots (2)$$

$$APD = \left(|X_i - MWR_i| / MWR_i \right) \times 100 \quad \dots (3)$$

where, X_i , represents the AOD at 500 nm retrieved from MFRSR, MTOPS or ESP.

The parameter MBD tells about the offset between two observations, whereas RMSD (equal to standard error for an unbiased estimation) gives an idea about the non-systematic component of the differences in measurements, as it is sensitive to extreme values. APD gives the information about the deviation in an observed value from the standard reference and is useful in quantifying the deviation in a set of measurements; however, lower values contribute disproportionately to APD.

Using the values of AOD for each concurrent pairs of observations, all these parameters were estimated and given in Table 2. The values in Table 2 clearly indicate that the mean APD and RMSD were lowest (6% and 0.03) in case of MWR-MFRSR observations, being highest in MWR-MTOPS (13% and 0.05); with MWR-ESP (8% and 0.04) in between. It was found that the computed APD between MWR and MFRSR was highest (~15) on 29 December 2008 when $\tau_{MWR} \sim 0.25$ and $\tau_{MFRSR} \sim 0.29$; and lowest (~ 0.9) on 17 February 2009 when $\tau_{MWR} \sim 0.47$ and $\tau_{MFRSR} \sim 0.48$. This indicates that the values of AOD retrieved from both MWR and MFRSR were in better agreement for highly turbid days compared to relatively moderate and low turbid days. Similar inference can be made from other two observations.

Table 2 — Statistical comparison of MWR retrieved AOD with other measurements

Parameter	MFRSR	MTOPS	ESP
Absolute percentage deviation (APD) (%)	6	13	8
Root mean square difference (RMSD)	0.03	0.05	0.04
Mean bias difference (MBD)	0.02	0.03	0.01
Regression coefficient (R)	0.99	0.86	0.92

However, it is important to note that in some of the cases when AOD are of the order of 0.01 (below the limits of instrumental uncertainty), APD can be 100% due to the weight that the low AOD contributes to APD. The lower values of RMSD (< 0.05) also establish the consistency of MWR observations with the others.

The values of MBD (~ 0.02, 0.03 and 0.01) between MWR-MFRSR, MWR-MTOPS and MWR-ESP observations pointed out the overestimation of MFRSR, MTOPS and ESP observations (τ_{MFRSR} , τ_{MTOPS} and τ_{ESP}) with respect to their counterpart (τ_{MWR}). The overestimation of MTOPS can be attributed to instantaneous sky conditions and observational period (e.g. discontinuity in some hours of measurements in a day) during its operation.

In addition to the above, the correlation coefficients for each pair of observations from the scatter plots of τ_{MWR} vs τ_{MFRSR} , τ_{MTOPS} and τ_{ESP} , has been estimated as shown in Fig. 3(a-c), with the orthogonal bars through the mean representing the standard deviations. The dotted line is the one corresponding to ideal one-to-one correlation between the two measurements. The linear least squares fit for each case are expressed as:

$$\tau_{MFRSR} = 0.92 \times \tau_{MWR} + 0.05 \quad \dots (4)$$

$$\tau_{MTOPS} = 0.98 \times \tau_{MWR} + 0.03 \quad \dots (5)$$

$$\tau_{ESP} = 0.91 \times \tau_{MWR} + 0.03 \quad \dots (6)$$

The pragmatic slopes [Eqs (4-6)] of 0.92, 0.98 and 0.91 with intercepts 0.05, 0.03 and 0.03, respectively for MFRSR, MTOPS and ESP against MWR AOD brought out again the fair accord between each pair of observations, with minor overestimation by other instruments compared to MWR. Very good correlation is seen between MWR and other instruments with correlation coefficients of $R \sim 0.99$, 0.86 and 0.92 for MFRSR, MTOPS and ESP, respectively. These are also shown in Table 2 along with the other statistical parameters. The differences in instrumental specifications and error calculations may lead to the scattered points in the fits. It is also quite evident from Fig. 3 that in most of the cases, MWR AODs are within the limit of standard deviations of MFRSR, MTOPS or ESP derived AODs. This implies that statistically the MWR is consistent with commercial instruments on a climatological scale.

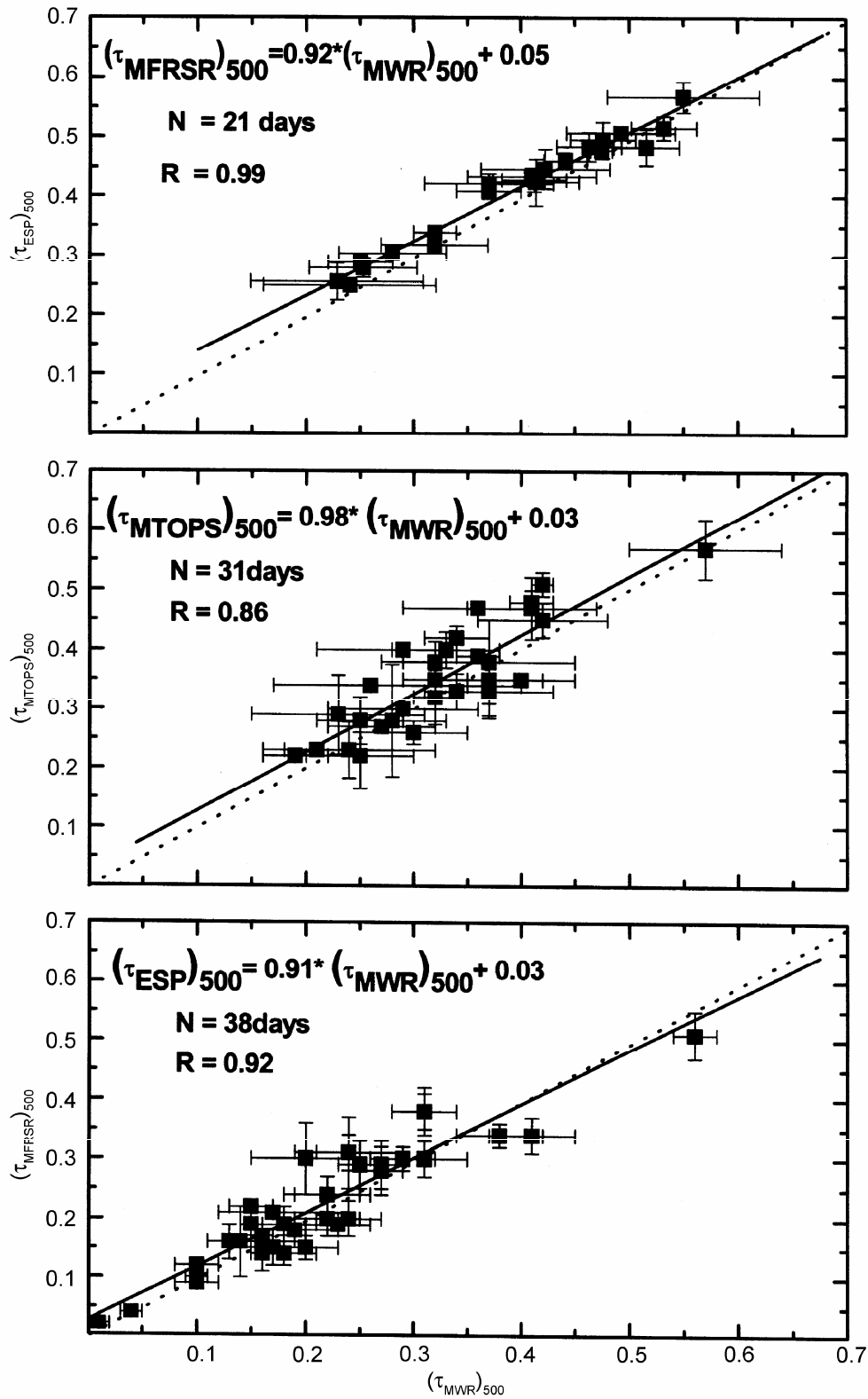


Fig. 3 — Inter-comparison of AODs at 500 nm retrieved from: (a) MWR [$(\tau_{MWR})_{500}$] and MFRSR [$(\tau_{MFRSR})_{500}$]; (b) MWR [$(\tau_{MWR})_{500}$] and MTOPS [$(\tau_{MTOPS})_{500}$]; and (c) MWR [$(\tau_{MWR})_{500}$] and ESP [$(\tau_{ESP})_{500}$]. Orthogonal bars indicate the standard deviations of the mean

5 Summary

The AOD at 500 nm retrieved from MWR observations were inter-compared with the concurrent measurements of three other commercially available instruments, which reveals the following:

- MWR and MFRSR retrieved AODs were well correlated with a correlation coefficient of $R \sim 0.99$. The retrievals were in fine accord with a mean bias of 0.02 and the absolute percentage deviation of 6% between the two measurements.
- The estimated AODs from MWR and MTOPS showed absolute percentage deviation of 13% with mean bias of 0.03 and a correlation coefficient of $R \sim 0.86$. This is the poorest but perhaps is still acceptable agreement between the two observations.
- A correlation coefficient of $R \sim 0.92$ implied fair consistency between the MWR and ESP retrieved AOD. A mean bias of 0.01 and absolute percentage deviation of 8% supported the consistency.

References

- 1 McComiskey A, Schwartz S E, Schmid B, Guan H, Lewis E R, Ricchiazzi P & Ogren J A, Direct aerosol forcing: Calculation from observables and sensitivity to inputs, *J Geophys Res (USA)*, 113 (2008) D09202.
- 2 Ackerman T P & Stokes G, The Atmospheric Radiation Measurement Program, *Phys Today (USA)*, 56 (2003) pp 38-45.
- 3 Augustine J A, Hodges G B, Cornwall C R, Michalsky J J & Medina C I, An update on SURFRAD — The GCOS Surface Radiation budget network for the continental United States, *J Atmos Ocean Technol (USA)*, 22 (2005) pp 1460–1472.
- 4 Holben B N, Eck T F, Slutsker I, Tanré D, Buis J P, Setzer A, Vermote E, Reagan J A, Kaufman Y J, Nakajima T, Lavenue F, Jankowiak I & Smirnov A, AERONET – A federated instrument network and data archive for aerosol characterization, *Remote Sens Environ (USA)*, 66 (1998) pp 1–16.
- 5 Schmid B, Michalsky J, Halthorne R, Beauharnois M, Harrison L, Livingston J, Russell P, Holben B, Eck T & Smirnov A, Comparison of aerosol optical depth from four solar radiometers during the fall 1997 ARM intensive observation period, *Geophys Res Lett (USA)*, 2617 (1999) pp 2725–2728.
- 6 Alexandrov M D, Lacis A A, Carlson B E & Cairns B, Characterization of atmospheric aerosols using MFRSR measurements, *J Geophys Res (USA)*, 113 (2008) D08204.
- 7 McArthur L J B, Halliwell D H, Niebergall O J, O’Neill N T, Slusser J R & Wehrli C, Field comparison of network Sun photometers, *J Geophys Res (USA)*, 108 (D19) (2003) 4596.
- 8 Yu H, Quinn P K, Feingold G, Remer L A, Kahn R A, Chin M & Schwartz S E, Remote sensing and in situ measurements of aerosol properties, burdens, and radiative forcing, in *Atmospheric Aerosol Properties and Climate Impacts, A Report by the U S Climate Change Science Program and the Subcommittee on Global Change Research*, Mian Chin, Ralph A Kahn & Stephen E Schwartz, eds, (National Aeronautics and Space Administration, Washington, DC, USA), 2009.
- 9 Moorthy K K, Saha A, Prasad B S N, Niranjan K, Jhurry D & Pillai P S, Aerosol optical depths over peninsular India and adjoining oceans during the INDOEX campaigns: Spatial, temporal and spectral characteristics, *J Geophys Res (USA)*, 106 (2001) pp 28539-28554.
- 10 Shaw G E, Reagan J A, Herman B M, Investigations of atmospheric extinction using direct solar radiation measurements made with a multiple wavelength radiometer, *J Appl Meteorol (USA)*, 12 (1973) pp 374-380.
- 11 Alexandrov M D, Lacis A A, Carlson B E & Cairns B, Remote sensing of atmospheric aerosols and trace gases by means of Multi Filter Rotating Shadowband Radiometer Part I: Retrieval algorithm, *J Atmos Sci (USA)*, 59 (2002) pp 524–543.
- 12 Alexandrov M D, Lacis A A, Carlson B E & Cairns B, Remote sensing of atmospheric aerosols and trace gases by means of Multi Filter Rotating Shadow band Radiometer Part II: Climatological applications, *J Atmos Sci (USA)*, 59 (2002) pp 544–566.
- 13 Alexandrov M D, Kiedron P, Michalsky J J, Hodges G, Flynn C J & Lacis A A, Optical depth measurements by shadowband radiometers and their uncertainties, *Appl Opt (USA)* 33 (2007) pp 8027-8038.
- 14 Michalsky J J, Schlemmer J A, Berkheiser W E, Berndt J L, Harrison L C, Laulainen N S, Larson N R & Barnard J C, Multi-year measurements of aerosol optical depth in the Atmospheric Radiation Measurement and Quantitative Links programs, *J Geophys Res (USA)*, 106 (2001) pp 12,099-12,107.
- 15 Morys M, Mims F M, Hagerup S, Anderson S E, Baker A, Kia J & Walkup T, Design, calibration and performance of MICROTOS II hand-held ozone monitor and Sun Photometer, *J Geophys Res (USA)* 106 (2001) pp 14,573–14,582.
- 16 Ichoku Charles, Robert Levy, Kaufman Y J *et al.*, Analysis of the performance characteristics of the five-channel Microtops II Sun Photometer for measuring aerosol optical thickness and perceptible water vapor, *J Geophys Res (USA)*, 107 (2002) D13, doi: 10.1029/2001JD00130.
- 17 Moorthy K K, Saha A, Niranjan K & Pillai P S, Optical properties of atmospheric aerosols over the Arabian Sea and Indian Ocean: North-south contrast across the ITCZ, *Curr Sci (India)*, 76 (1999) pp 956-960.